

## FULL PAPER

# Green synthesis of supported palladium nanoparticles employing pine needles as reducing agent and carrier: New reusable heterogeneous catalyst in the Suzuki coupling reaction

Guanghui Liu<sup>1</sup> | Xuefeng Bai<sup>1,2\*</sup> | Hongfei Lv<sup>2</sup>

<sup>1</sup> School of Chemistry and Material Sciences, Heilongjiang University, Harbin 150080, China

<sup>2</sup> Institute of Petrochemistry, Heilongjiang Academy of Sciences, Harbin 150040, China

**Correspondence**

Xuefeng Bai, School of Chemistry and Material Sciences, Heilongjiang University, Harbin 150080, China.

Email: tommybai@126.com

A green method for the synthesis of supported Pd nanoparticles (NPs) using pine needle extract as the reducing agent and the extracted residue of pine needle (RPN) as the carrier is described. The Pd/RPN nanocomposites were characterized using Fourier transform infrared, UV–visible, inductively coupled plasma atomic emission and X-ray photoelectron spectroscopies, transmission electron microscopy and X-ray diffraction. The spherical Pd NPs had a mean particle size of 3.25 nm and were evenly distributed on the RPN surface. More importantly, the Pd/RPN nanocomposite, as a heterogeneous catalyst, presented superior catalytic activity for the Suzuki coupling reaction. The yield of the reaction of 4-bromotoluene with phenylboronic acid catalyzed by Pd<sub>0.03</sub>/RPN reached 98% with low Pd loading (0.1 mmol%) at room temperature for 30 min. In addition, the catalyst could be easily separated by centrifugation and reused at least six times without significant loss of activity.

**KEYWORDS**

green synthesis, heterogeneous catalyst, Pd nanoparticles, pine needles, Suzuki coupling reaction

## 1 | INTRODUCTION

The Suzuki coupling reaction is a powerful and straightforward reaction in the field of organic synthesis due to its wide application for the selective construction of C–C bonds to synthesize biphenyl compounds,<sup>[1–4]</sup> such as in natural products,<sup>[5,6]</sup> liquid crystalline polymers,<sup>[7,8]</sup> nonlinear optical materials<sup>[9,10]</sup> and pharmaceuticals.<sup>[11]</sup>

Traditionally, homogeneous Pd catalysts can form complexes with phosphine ligands or other protective agents, such as polyvinylpyrrolidone and cetyltrimethylammonium bromide,<sup>[12,13]</sup> to produce water-soluble catalysts, which are generally applied in the Suzuki coupling reaction and exhibit excellent catalytic activity.<sup>[14–16]</sup> However, many of these chemical agents may cause serious problems to the environment due to their toxicity and lead to high production costs. The separation of catalyst from reaction system and the reuse of the catalysts in consecutive reactions are the major limitations for the application of these catalytic systems.

Heterogeneous catalysts are preferred over homogeneous catalysts due to their facile separation from a reaction mixture and the possibility of recycling.<sup>[17–19]</sup> Supported Pd catalysts play an important role in a lot of catalytic reactions, especially in the Suzuki coupling reaction. However, there are many shortcomings, such as aggregation and leaching of Pd nanoparticles (NPs) on the surface of supports, which result in a low Pd utilization efficiency. One solution to this problem is to uniformly disperse Pd NPs on the surface of supports, such as microporous polymers,<sup>[20]</sup> nano-silica,<sup>[21]</sup> TiO<sub>2</sub><sup>[22]</sup> or carbon materials.<sup>[23,24]</sup>

The synthesis of Pd NPs is generally carried out using chemical agents or advanced technical equipment, which are harmful to the environment and increases the cost of production. In recent years, the utilization of biosynthetic techniques for the preparation of metal NPs has emerged as a new and reliable method due to a growing need to develop eco-friendly processes in nanomaterial synthesis.<sup>[25–27]</sup> Extensive work has been committed to the green synthesis

of metal NPs, employing bacteria,<sup>[28–31]</sup> fungi<sup>[25,32–34]</sup> and plants.<sup>[35–37]</sup> According to these studies, a biosynthetic method using plants has emerged as a viable alternative to traditional chemical and physical processes, it being simple, cost-effective, safe and eco-friendly. To date, there is no report on the synthesis of supported metal NPs using plants as the reducing agent and carrier.

Pine is an evergreen plant of the Pinaceae family located throughout the world (Figure 1). The main classes of secondary metabolites occurring in pine needles are polyphenolic compounds, such as tannins,  $\alpha$ -pinene, *trans*-caryophyllene,  $\alpha$ -terpineol, terpinene-4-ol and  $\delta$ -cadinene.<sup>[38,39]</sup> Accordingly, there are compounds with potential antioxidant activity in this plant. Thus, the plant can serve as an effective and green source for the reduction of Pd ions for the synthesis of metal Pd NPs. In addition, the foliage is composed of a cellulose structure,<sup>[40]</sup> which is rich in hydroxyl groups and can be combined with metal NPs. Therefore, it can serve as a good carrier for supported Pd NPs.

In this paper, an eco-friendly and economic process for the synthesis of supported Pd NPs using pine needles as the reducing agent and carrier is reported. In addition, the catalytic activity of nanocomposites of Pd and extracted residue of pine needle (RPN), used as a reusable heterogeneous catalyst, was further investigated in the Suzuki coupling reaction.

## 2 | EXPERIMENTAL

### 2.1 | Instrumentation and Reagents

Pine needles were collected from Harbin (northeastern China). All chemicals were purchased from Tianjin Kermel and Sinopharm Chemical Reagent Co. Ltd. All chemicals were used without further purification. UV–visible spectroscopy was performed with a UV-2450 (Shimadzu). Powder X-ray diffraction (XRD) analyses were conducted



FIGURE 1 Image of pine needles

with a Bruker D8 Advance diffractometer equipped with Cu K $\alpha$  radiation. Transmission electron microscopy (TEM) was conducted with a JEM-2100FX (200 kV). Inductively coupled plasma atomic emission spectrometry (ICP-AES) was carried out with an ICP-7510 (Shimadzu). Fourier transform infrared (FT-IR) spectra was recorded with an Avatar Nicolet 6700 using pressed KBr pellets with a scanning range from 500 to 4000  $\text{cm}^{-1}$ . X-ray photoelectron spectroscopy (XPS) was conducted with a Kratos AXIS ULTRA DLD spectrometer with Al X-ray source.

### 2.2 | Preparation of Pine Needle Extract (PNE) and RPN

Sundried pine needles were milled. Then, 2 g of the powder was added into 100 ml of deionized water and refluxed at 60°C for 1 h. The PNE obtained was centrifuged at 4000 rpm and filtered through Whatman No. 1 filter paper. The filtrate was collected in an Erlenmeyer flask and stored at 4°C for further use. The filter residue was RPN.

### 2.3 | Preparation of Pd/RPN Catalyst

To prepare the Pd/RPN catalyst with 3 wt% Pd, 0.2 g of RPN was added into 6 ml of  $\text{Na}_2\text{PdCl}_4$  solution (0.01 M) and impregnated for 12 h at room temperature. Subsequently, 10 ml of PNE was added dropwise to this mixture with magnetic stirring at 60°C for 3 h. The product, denoted as Pd<sub>0.03</sub>/RPN, was separated using a centrifugation step. The separated solid was washed two times using deionized water. For comparison, Pd<sub>0.01</sub>/RPN, Pd<sub>0.05</sub>/RPN and Pd<sub>0.10</sub>/RPN nanocomposites were also prepared under the same conditions.

### 2.4 | Catalytic Suzuki Coupling Reaction

Under air atmosphere, aryl halide (1 mmol),  $\text{K}_2\text{CO}_3$  (2 mmol) and the catalyst (0.1 mmol%) were added into a mixed solvent of 15 ml of EtOH–H<sub>2</sub>O (1:1) with constant stirring at room temperature for 10 min to obtain an evenly dispersed system. Then, phenylboronic acid (1.5 mmol) was added into the mixture. After completion of the reaction, the mixture (5 ml) was added to 5 ml of NaOH solution (0.2 mol l<sup>-1</sup>) and extracted two times with EtOAc (10 ml). The combined organic layers were collected and dried in air to obtain the crude product. Subsequently, the obtained products were determined using HPLC analysis.

### 2.5 | Catalyst Recycling Experiment

After the reaction, the catalyst was collected by centrifugation. The separated solid was washed three times using NaOH solution (0.2 mol l<sup>-1</sup>) to remove the absorbed phenylboronic acid. Next, the collected solid was washed with ethyl acetate and dried under vacuum. Subsequently, the recovered catalyst was used for another run.

### 3 | RESULTS AND DISCUSSION

#### 3.1 | UV-Visible Analysis

As shown in Figure 2, the UV-visible spectrum of PNE exhibits a peak at 276 nm, which is in accordance with the absorption of the gallic acid system. It is related to  $\pi$ - $\pi^*$  transitions and indicates that polyphenol compounds are present in the extract. The absorption spectra of Pd colloidal suspensions of various Pd loadings, which were treated for 3 h, are also shown. The absorption of  $\text{Na}_2\text{PdCl}_4$  solution was used as a reference for comparison. The absorption bands present in the reference sample spectrum are attributed to the characteristic absorption of  $\text{PdCl}_4^{2-}$  species.<sup>[41]</sup> The absence of absorption peak above 420 nm for all of the samples indicates that the initial bivalent Pd species is adequately reduced to zero-valent Pd (Figure 2a). During the reduction process, the color of the PRN changes from light yellow to deep black (Figure 2b).

#### 3.2 | TEM and ICP-AES Analyses

In Figure 3, the TEM images further confirm the size and morphology of the Pd NPs, which are dispersed on the RPN surface. With low Pd loading ( $\text{Pd}_{0.01}/\text{RPN}$ ), spherical Pd NPs with an average particles size of 5.25 nm are quantitatively sparse on the RPN surface (Figure 3a, b). At the appropriate Pd loading ( $\text{Pd}_{0.03}/\text{RPN}$  and  $\text{Pd}_{0.05}/\text{RPN}$ ), the spherical Pd nanoparticles are evenly dispersed on the RPN surface (Figure 3c, e). According to the particle size distribution histograms, the average particle size of  $\text{Pd}_{0.03}/\text{RPN}$  is 3.25 nm (Figure 3d), which is smaller than that of  $\text{Pd}_{0.05}/\text{RPN}$  (5.18 nm; Figure 3f). The high-resolution TEM (HRTEM) image further manifests that the Pd crystal plane is 0.224 nm (inset of Figure 3c), which corresponds to the lattice spacing of the (111) plane of metal Pd.<sup>[42]</sup> As shown in Figure 3g, with high Pd loading ( $\text{Pd}_{0.10}/\text{RPN}$ ), Pd NPs with triangular, cubic and rod structures are formed. This may be due to the lack of biomolecules acting as stabilizing agents, so that mostly non-spherical nanoparticles are

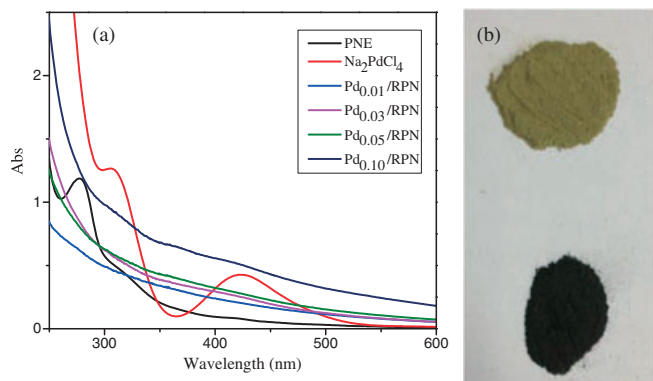


**FIGURE 2** (A) UV-visible spectra of PNE,  $\text{Na}_2\text{PdCl}_4$  solution and Pd NP suspensions with various Pd loadings after 3 h. (B) Color change of RPN before and after the reaction

obtained in these samples. From the size distribution histograms, when the Pd load is increased to 10%, the average particle size is increased to 11.52 nm (Figure 3h). The results reveal that the Pd/RPN nanocomposites have been successfully synthesized and the small Pd NPs are highly distributed on the RPN without any agglomeration at appropriate Pd loadings (3 wt% Pd loads). The actual amount of Pd in  $\text{Pd}_{0.03}/\text{RPN}$  determined using ICP-AES is 2.72 wt%.

#### 3.3 | XRD Analysis

XRD patterns of the as-prepared Pd/RPN are shown in Figure 4. The peak intensities of the Pd/RPN nanocomposites with low Pd loads are not obvious (Figure 4a, b). In combination with the TEM analysis, this may be due to the relatively broad reflections, indicating quantitatively sparse or small particles size. This suggests that no characteristic peaks of metallic Pd are observed using XRD up to a Pd load of 5 wt%. Only an obvious (111) peak of metallic Pd is observed at  $2\theta = 40.1^\circ$  (Figure 4c). Upon increasing the Pd load to 10 wt% (Figure 4d), peaks located at  $40.1^\circ$ ,  $46.1^\circ$  and  $67.9^\circ$  are observed, which are indexed to the (111), (200) and (220) Bragg reflections, respectively, of the face-centered cubic structure of Pd (JPDs 87-0643).<sup>[43]</sup>

#### 3.4 | XPS Analysis

In Figure 5(a), the XPS survey spectrum of  $\text{Pd}_{0.03}/\text{RPN}$  shows that Pd/RPN nanocomposite consists of C, N, O and Pd. The XPS spectrum of the Pd 3d region (Pd 3d<sub>5/2</sub> and Pd 3d<sub>3/2</sub>) consists of four peaks (Figure 5b); the peaks at 335.3 and 340.5 eV belong to  $\text{Pd}^0$ , and the other peaks at 337.1 and 342.2 eV are assigned to  $\text{Pd}^{2+}$ .<sup>[44]</sup> On the basis of peak area analysis, zero-valent Pd in  $\text{Pd}_{0.03}/\text{RPN}$  amounts to 65%. A possible reason for the presence of  $\text{Pd}^{2+}$  is that the reduction of  $\text{Pd}^{2+}$  does not proceed to completion during the fabrication. Another reason is that the exposed zero-valent Pd can be further oxidized into divalent Pd at ambient conditions.

#### 3.5 | FT-IR Analysis

As shown in Figure 6a, the prominent absorption peaks for PNE appear at 3415, 2923, 1627, 1515, 1405, 1262 and 1074  $\text{cm}^{-1}$ . Generally, the broad peak at 3415  $\text{cm}^{-1}$  is attributed to the O-H (phenolic) stretch. The peaks at 1627, 1515, 1405, 1262 and 1074  $\text{cm}^{-1}$  are assigned to the stretching vibrations of (NH)-C=O (protein), C=C (aromatic), C-O-C (esters, ethers) and C-OH/C-H (polyols), respectively. Based on this analysis, the polyphenol compounds, with -OH groups, can be used as a reducing agent for the reduction  $\text{Pd}^{2+}$  to synthesize Pd NPs. And the protein compounds, with (NH)-C=O groups, can serve as a stabilizing agent for protecting the Pd NPs. Comparing the FT-IR spectra of RPN and  $\text{Pd}_{0.03}/\text{RPN}$  (Figure 6b), there is no noticeable change in the characteristic absorption peaks,

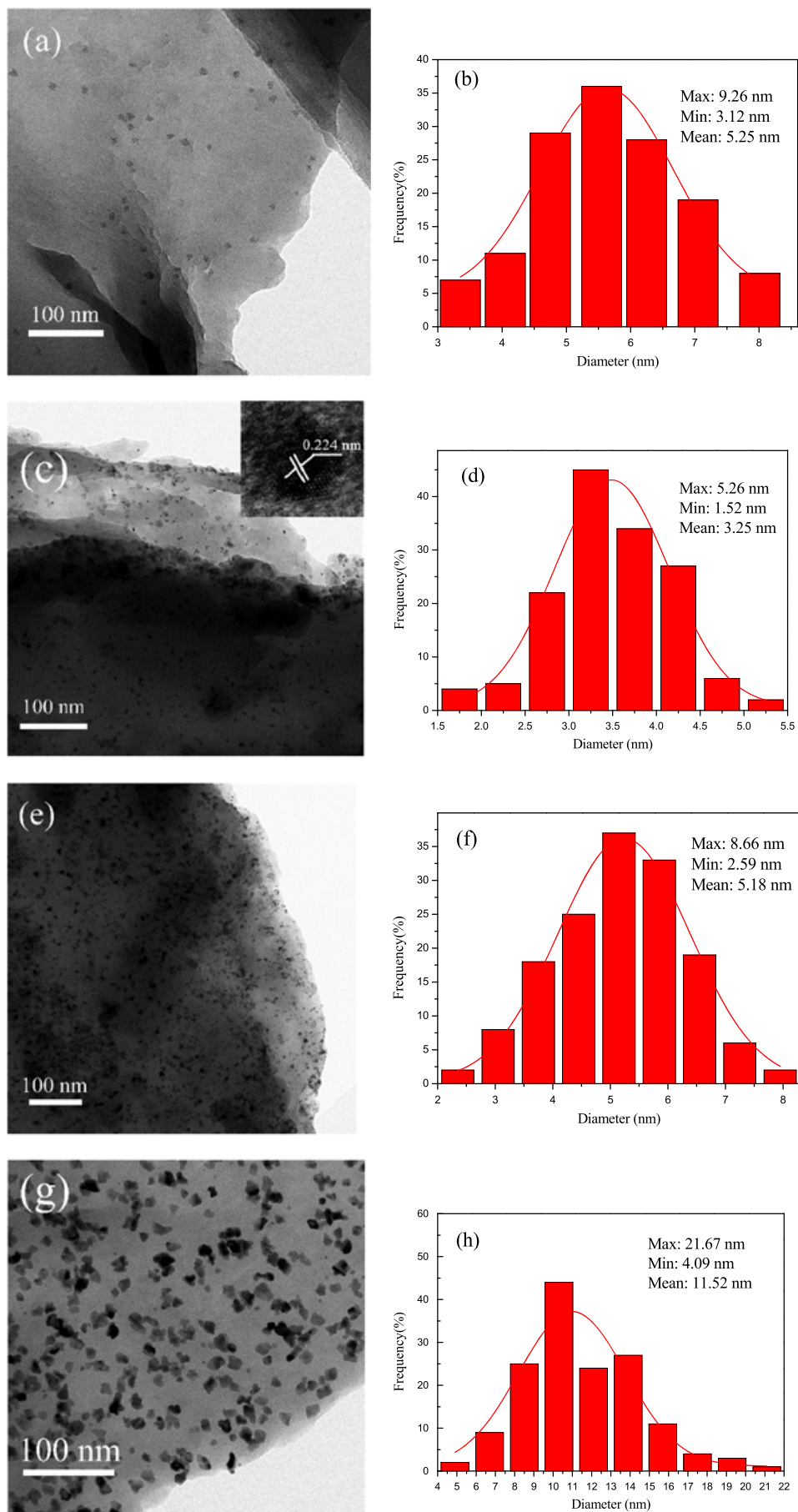


**FIGURE 3** (a) TEM image and (b) size distribution of Pd<sub>0.01</sub>/RPN; (c) TEM image (inset: HRTEM image) and (d) size distribution of Pd<sub>0.03</sub>/RPN; (e) TEM image and (f) size distribution of Pd<sub>0.05</sub>/RPN; (g) TEM image and (h) size distribution of Pd<sub>0.10</sub>/RPN

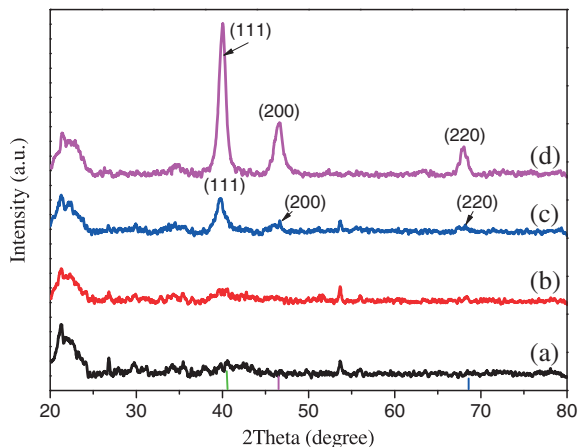


**FIGURE 4** XRD patterns of (a) Pd<sub>0.01</sub>/RPN, (b) Pd<sub>0.03</sub>/RPN, (c) Pd<sub>0.05</sub>/RPN and (d) Pd<sub>0.10</sub>/RPN

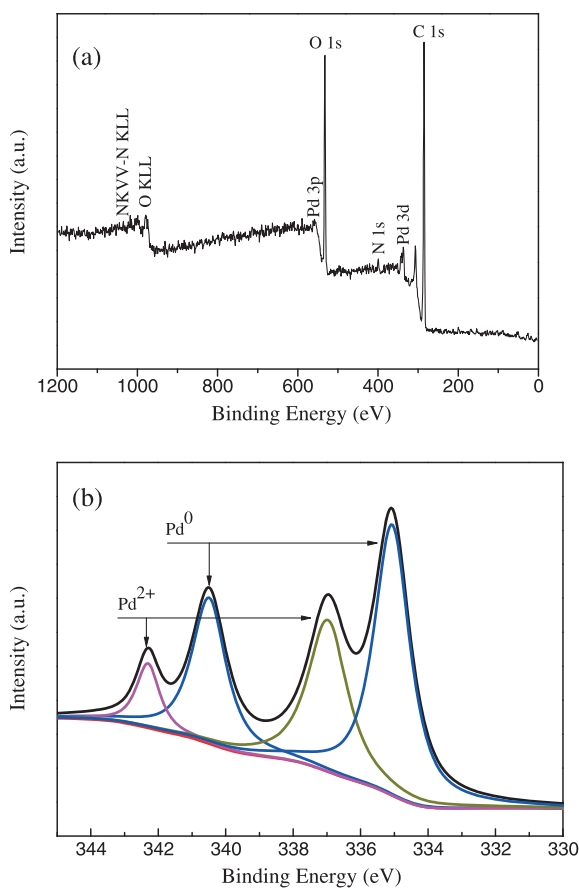


**FIGURE 5** (a) XPS survey spectrum of Pd<sub>0.03</sub>/RPN; (b) Pd 3d core-level XPS spectrum

which indicates that there is a non-covalently coupled interaction between the Pd species and RPN in the Pd/RPN nanocomposites.

### 3.6 | Catalytic Activity Evaluation

The Suzuki coupling reaction of 4-bromotoluene with phenylboronic acid (Scheme 1) was used to compare the

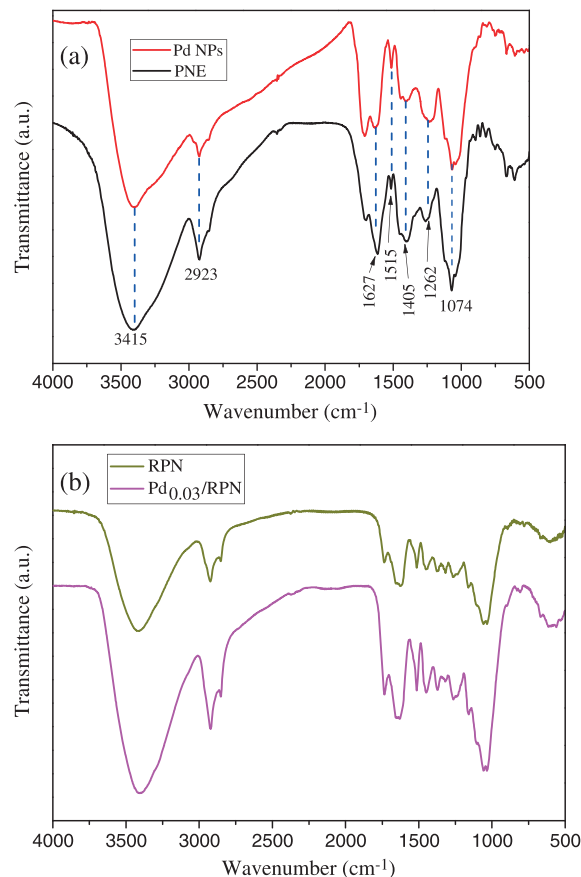
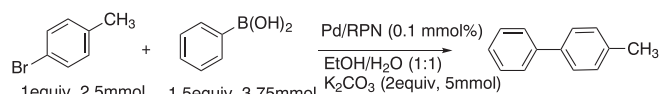


**FIGURE 6** FT-IR spectra: (a) PNE and Pd NPs; (b) RPN and Pd<sub>0.03</sub>/RPN



**SCHEME 1** Suzuki reaction catalyzed by Pd/RPN

catalytic performance of the synthesized Pd/RPN complexes (1, 3, 5, or 10 wt%). The reaction was carried out under rather mild conditions, using EtOH–H<sub>2</sub>O (1:1) as the solvent and K<sub>2</sub>CO<sub>3</sub> as the base at room temperature under an air atmosphere in the presence of a low amount of catalyst (0.1 mmol%).

Figure 7 shows the yields of biphenyl at different intervals with various catalysts. Among all the catalysts with different Pd loads, Pd<sub>0.03</sub>/RPN exhibits the best catalytic activity; the yield of the reaction of 4-bromotoluene with phenylboronic acid reaches 98% with 0.1 mmol% catalyst at room temperature for 30 min. Lower catalytic activity is obtained with higher Pd load (10 wt%) and lower Pd load (1 wt%), due to the increase of the particle size and reduction of the degree of dispersion, respectively. The results are also supported by the TEM analysis. Therefore, the dispersion and size uniformity are the key factors determining the activity of catalyst. This result may be attributed to the relatively strong interaction between the Pd species and RPN in the Pd/RPN nanocomposites.

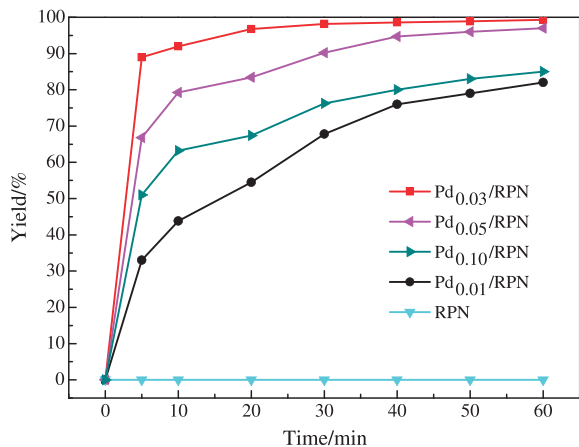


FIGURE 7 Yields of biphenyl at different intervals with various catalysts

To survey the substrate generality for  $\text{Pd}_{0.03}/\text{RPN}$  catalyst, the general applicability of the coupling reaction between aryl halide and phenylboronic acid was studied, and the results are summarized in Table 1. Various *p*-substituted aryl bromides, containing either electron-donating groups (Table 1, entries 1 and 4) or electron-withdrawing groups (Table 1, entries 2 and 3), undergo the coupling reaction smoothly and produce the corresponding products with excellent yields. The *m*-substituted nitrobenzene (Table 1, entry 5) also gives the corresponding product with a high yield. The *o*-substituted aryl bromides (Table 1, entries 6 and 7) give the corresponding products in poor yields due to steric effects. The substrate scope was further extended to aryl chlorides (Table 1, entries 8 and 9). Poor yields are observed even after prolonging the reaction times to 6 h.

The reusability and stability of a catalyst are essential from an economic standpoint and for industrial applications. As evident from Table 2, the  $\text{Pd}_{0.03}/\text{RPN}$  catalyst can be recycled simply using a centrifugation step. In addition, although the yield gradually reduces, a yield of 84% is still obtained in the sixth cycle. After six recycles, the amount

TABLE 1 Suzuki coupling reactions of various aryl halides with phenylboronic acid<sup>a</sup>

Entry	R	X	Time (min)	Yield (%)
1	4-CH <sub>3</sub>	Br	30	98
2	4-NO <sub>2</sub>	Br	30	97
3	4-CN	Br	30	92
4	4-OCH <sub>3</sub>	Br	30	98
5	3-NO <sub>2</sub>	Br	30	96
6	2-CH <sub>3</sub>	Br	30	68
7	2-OCH <sub>3</sub>	Br	30	28
8	H	Cl	360	46
9	4-NO <sub>2</sub>	Cl	360	34

<sup>a</sup>Reaction conditions: aryl halide (1 mmol), phenylboronic acid (1.5 mmol),  $\text{K}_2\text{CO}_3$  (2 mmol),  $\text{Pd}_{0.03}/\text{RPN}$  (0.1 mmol%), EtOH–H<sub>2</sub>O (6 ml/6 ml) at room temperature.

TABLE 2 Recycling study of  $\text{Pd}_{0.03}/\text{RPN}$ <sup>a</sup>

Run	1	2	3	4	5	6
Yield (%)	98	96	93	91	89	84

<sup>a</sup>Reaction conditions: 4-bromotoluene (1 mmol), phenylboronic acid (1.5 mmol),  $\text{Pd}_{0.03}/\text{RPN}$  (0.1 mmol%),  $\text{K}_2\text{CO}_3$  (2 mmol), ethanol–H<sub>2</sub>O (6 ml/6 ml) at room temperature for 30 min.

of Pd in the  $\text{Pd}_{0.03}/\text{RPN}$  determined using ICP-AES is 1.98 wt%.

## 4 | CONCLUSIONS

In summary, an effective and reusable Pd/RPN catalyst was designed and successfully prepared via a low-cost and green method using PNE as the reducing agent and RPN as the carrier. Pd NPs with small size and highly dispersed were successfully prepared at appropriate Pd loading (3 wt%). The  $\text{Pd}_{0.03}/\text{RPN}$  catalyst demonstrated excellent catalytic performance for the Suzuki coupling reaction and could be reused at least six times without significant loss of activity. The excellent catalytic activity can be attributed to the close interaction between the Pd NPs and abundant hydroxyl groups on the surface of RPN, which is beneficial for obtaining well-dispersed and small Pd NPs. This method provides a simple and eco-friendly route for the synthesis supported Pd NPs, which will find potential application in other nanometal materials.

## ACKNOWLEDGMENTS

This project was financially supported by the National Natural Science Foundation of China no. 21276067, NSFC-RFBR no. 214111301884, Program of International S&T cooperation no. 2013DFR40570 and Science Foundation of Heilongjiang Academy of Sciences.

## REFERENCES

- [1] A. Suzuki, *J. Organometal. Chem.* **1999**, 576, 147.
- [2] T. X. Zhang, Z. Li, *Comput. Theor. Chem.* **2013**, 1016, 28.
- [3] C. Xu, X. Q. Hao, Z. Q. Xiao, Z. Q. Wang, X. E. Yuan, W. J. Fu, B. M. Ji, M. P. Song, *J. Org. Chem.* **2013**, 78, 8730.
- [4] P. D. Thornton, N. Brown, D. Hill, B. Neuenswander, G. H. Lushington, C. Santini, K. R. Buszek, *Abstr. Pap. Am. Chem. Soc.* **2012**, 244.
- [5] M. C. Kozlowski, B. J. Morgan, E. C. Linton, *Chem. Soc. Rev.* **2009**, 38, 3193.
- [6] X. Shen, G. O. Jones, D. A. Watson, B. Bhayana, S. L. Buchwald, *J. Am. Chem. Soc.* **2010**, 132, 11278.
- [7] M. Suzuki, J. C. Lim, T. Saegusa, *Macromolecules* **1990**, 23, 1574.
- [8] Z. Bao, Y. Chen, R. Cai, L. Yu, *Macromolecules* **1993**, 26, 5281.
- [9] A. Yokoyama, H. Suzuki, Y. Kubota, K. Ohuchi, H. Higashimura, T. Yokozawa, *J. Am. Chem. Soc.* **2007**, 129, 7236.
- [10] A. Yokoyama, H. Suzuki, Y. Kubota, K. Ohuchi, H. Higashimura, T. Yokozawa, *J. Am. Chem. Soc.* **2007**, 129, 7236.
- [11] L. Ackermann, S. Barfusser, J. Pospech, *Org. Lett.* **2010**, 12, 724.
- [12] R. Narayanan, M. A. El-Sayed, *J. Phys. Chem. B* **2004**, 108, 8572.
- [13] C. C. Wang, D. H. Chen, T. C. Huang, *Colloids Surf., A* **2001**, 189, 145.

- [14] N. T. Phan, M. Van Der Sluys, C. W. Jones, *Adv. Synth. Catal.* **2006**, *348*, 609.
- [15] A. Datta, K. Ebert, H. Plenio, *Organometallics* **2003**, *22*, 4685.
- [16] J. P. Wolfe, S. L. Buchwald, *Angew. Chem. Int. Ed.* **1999**, *38*, 2413.
- [17] Y. Kitamura, S. Sako, A. Tsutsui, Y. Monguchi, T. Maegawa, Y. Kitade, H. Sajiki, *Adv. Synth. Catal.* **2010**, *352*, 718.
- [18] S. W. Kim, M. Kim, W. Y. Lee, T. Hyeon, *J. Am. Chem. Soc.* **2002**, *124*, 7642.
- [19] T. Kang, Q. Feng, M. Luo, *Synlett* **2005**, *2005*, 2305.
- [20] K. Okumura, T. Tomiyama, S. Okuda, H. Yoshida, M. Niwa, *J. Catal.* **2010**, *273*, 156.
- [21] A. Fihri, D. Cha, M. Bouhrara, N. Almana, V. Polshettiwar, *ChemSusChem* **2012**, *5*, 85.
- [22] M. Nasrollahzadeh, S. M. Sajadi, *J. Colloid Interface Sci.* **2016**, *465*, 121.
- [23] C. Liu, X. Rao, Y. Zhang, X. Li, J. Qiu, Z. Jin, *Eur. J. Org. Chem.* **2013**, 4345.
- [24] X. Wang, Y. Tang, Y. Gao, T. Lu, *J. Power Sources* **2008**, *175*, 784.
- [25] M. Sastry, A. Ahmad, M. I. Khan, R. Kumar, *Curr. Sci.* **2003**, *85*, 162.
- [26] J. E. van de Mortel, L. A. Villanueva, H. Schat, J. Kwekkeboom, S. Coughlan, P. D. Moerland, E. V. L. van Themaat, M. Koornneef, M. G. Aarts, *Plant Physiol.* **2006**, *142*, 1127.
- [27] C. S. Cobbett, *Curr. Opin. Plant Biol.* **2000**, *3*, 211.
- [28] N. Yousefi, M. Pazouki, M. Alizadeh, F. A. Hesari, *Synth. React. Inorg. Met.-Org. Chem.* **2016**, *46*, 464.
- [29] J. A. Bennett, I. P. Mikheenko, K. Deplanche, I. J. Shannon, J. Wood, L. E. Macaskie, *Appl. Catal. B* **2013**, *140*, 700.
- [30] M. Eugenio, N. Mueller, S. Frases, R. Almeida-Paes, L. M. T. R. Lima, L. Lemgruber, M. Farina, W. de Souza, C. Sant'Anna, *RSC Adv.* **2016**, *6*, 9893.
- [31] Rahisuddin, S. A. Al-Thabaiti, Z. Khan, N. Manzoor, *Bioproc. Biosyst. Eng.* **2015**, *38*, 1773.
- [32] Y. Qian, H. Yu, D. He, H. Yang, W. Wang, X. Wan, L. Wang, *Bioproc. Biosyst. Eng.* **2013**, *36*, 1613.
- [33] Y. S. Chan, M. M. Don, *Mater. Sci. Eng. C* **2013**, *33*, 282.
- [34] C. Borelli, M. Schaller, M. Niewerth, K. Nocker, B. Baasner, D. Berg, R. Tiemann, K. Tietjen, B. Fugmann, S. Lang-Fugmann, H. C. Korting, *Chemotherapy* **2008**, *54*, 245.
- [35] M. Atarod, M. Nasrollahzadeh, S. M. Sajadi, *J. Colloid Interface Sci.* **2016**, *465*, 249.
- [36] M. Nasrollahzadeh, S. M. Sajadi, A. Rostami-Vartooni, M. Bagherzadeh, *J. Colloid Interface Sci.* **2015**, *448*, 106.
- [37] D. Baruah, R. N. Das, S. Hazarika, D. Konwar, *Catal. Commun.* **2015**, *72*, 73.
- [38] M. P. Kähkönen, A. I. Hopia, H. J. Vuorela, J. P. Rauha, K. Pihlaja, T. S. Kujala, M. Heinonen, *J. Agric. Food Chem.* **1999**, *47*, 3954.
- [39] K. Y. Kim, H. J. Chung, *J. Agric. Food Chem.* **2000**, *48*, 1269.
- [40] R. L. Parfitt, R. H. Newman, *Plant Soil* **2000**, *219*, 273.
- [41] X. Xie, G. Gao, Z. Pan, T. Wang, X. Meng, L. Cai, *Sci. Rep.* **2015**, *5*, 8515.
- [42] H. M. Song, B. A. Moosa, N. M. Khashab, *J. Mater. Chem.* **2012**, *22*, 15953.
- [43] F. Harraz, S. El-Hout, H. Killa, I. Ibrahim, *J. Catal.* **2012**, *286*, 184.
- [44] J. Moulder, W. Stickle, P. Sobol, K. Bomben, *Handbook of X-ray Photoelectron Spectroscopy*, Perkin-Elmer, Eden Prairie, MN **1992**.

**How to cite this article:** Liu, G., Bai, X., and Lv, H. (2016), Green synthesis of supported palladium nanoparticles employing pine needles as reducing agent and carrier: New reusable heterogeneous catalyst in the Suzuki coupling reaction, *Appl. Organometal. Chem.*, doi: 10.1002/aoc.3587